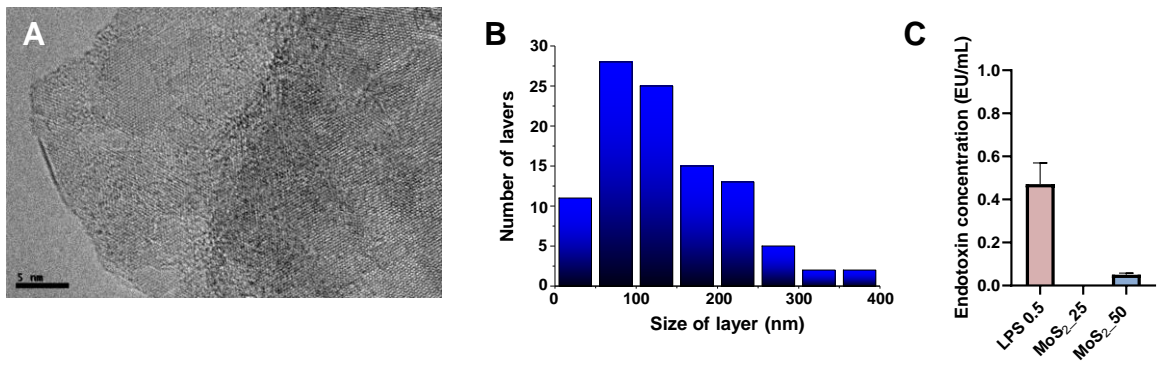


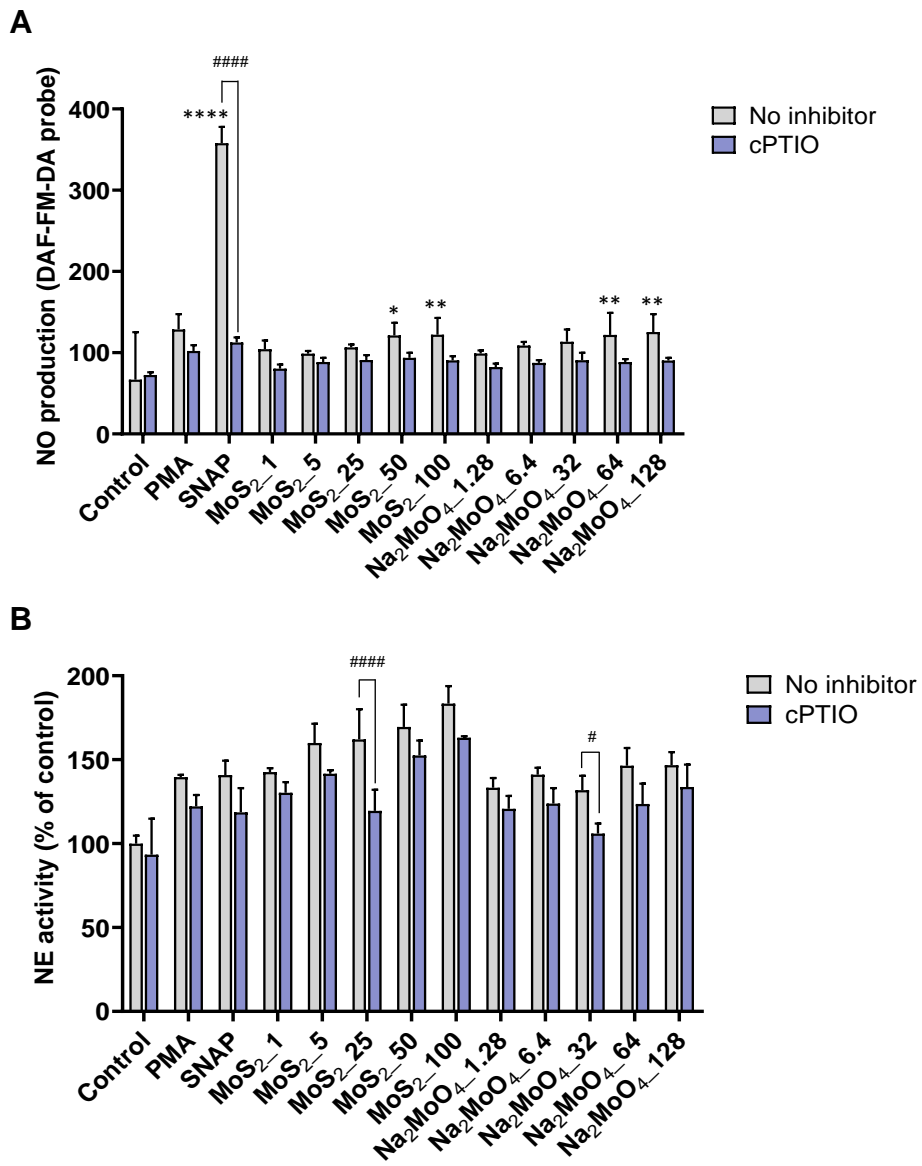
## Supporting Information

# **Two-dimensional molybdenum disulfide nanosheets evoke nitric oxide-dependent antibacterial effects**

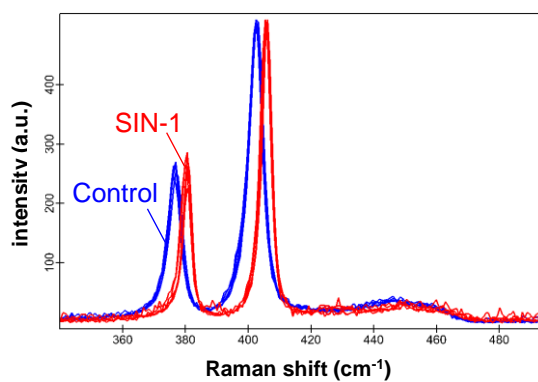
Guotao Peng, Viviana González, Ester Vázquez, Jon O. Lundberg, and Bengt Fadeel



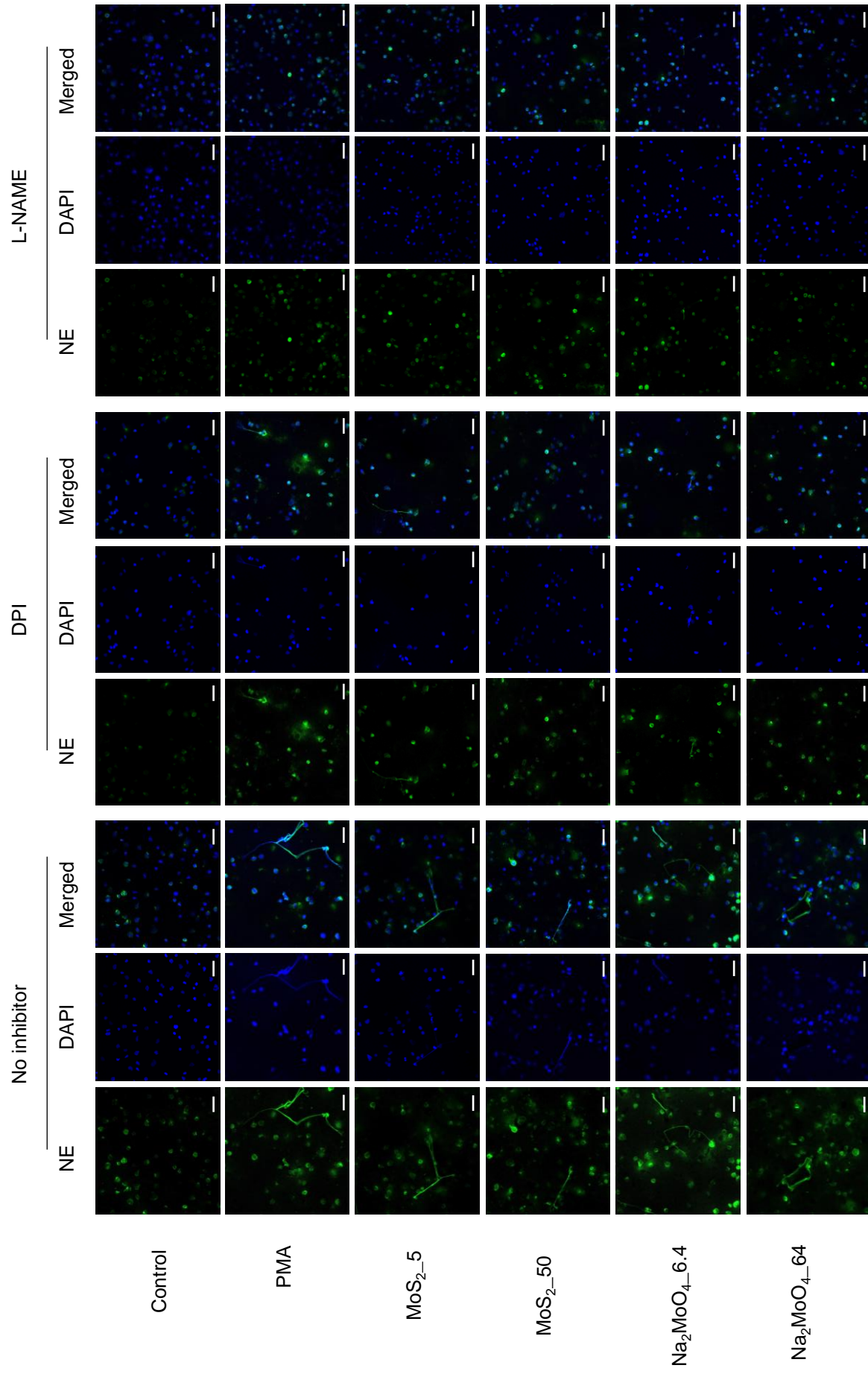
**Figure S1.** Physicochemical characterization of 2D MoS<sub>2</sub> nanosheets produced through mechanochemical exfoliation as described in: González et al., *Nanoscale Horizons*. 2020;5:331-335. (A) Representative TEM image of 2D-MoS<sub>2</sub>. (B) Lateral size distribution of MoS<sub>2</sub> nanosheets as determined by TEM. The average size was 136.00 ± 79.28 nm. (C) Endotoxin assessment of MoS<sub>2</sub> using the LAL assay. The endotoxin concentration at 25 µg/mL was undetectable and at 50 µg/mL it was 0.051 ± 0.007 EU/mL.



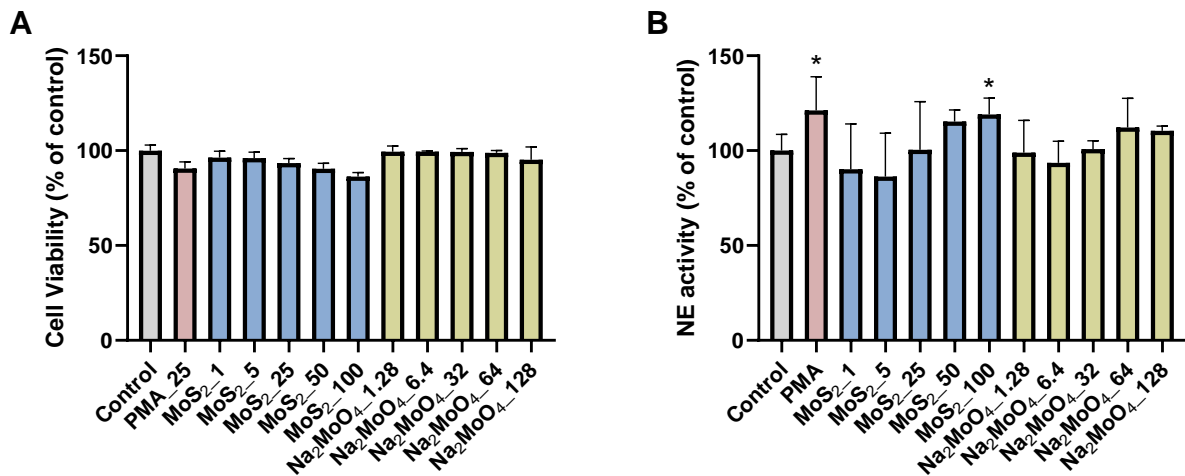
**Figure S2.** Role of NO for NET release. (A) Quantification of cellular NO production determined by DAF-FM-DA assay. Both MoS<sub>2</sub> and Na<sub>2</sub>MoO<sub>4</sub> led to the generation of NO in a dose-dependent manner after exposure for 3 h. The NO donor SNAP (500 μM) triggered an increase of NO and the NO scavenger cPTIO (250 μM) significantly suppressed NO production. Student's *t*-test was used for the statistical significance compared to controls (\*  $p < 0.05$ , \*\*  $p < 0.01$ , \*\*\*\*  $p < 0.0001$ ), as well as each condition with or without cPTIO (####  $p < 0.0001$ ). (B) The NO scavenger, cPTIO inhibited NET release, as determined by extracellular NE activity. Results are presented as mean values  $\pm$  S.D. of three independent experiments. Student's *t*-test was used for the statistical significance (#  $p < 0.05$ , ####  $p < 0.0001$ ).

**A****B**

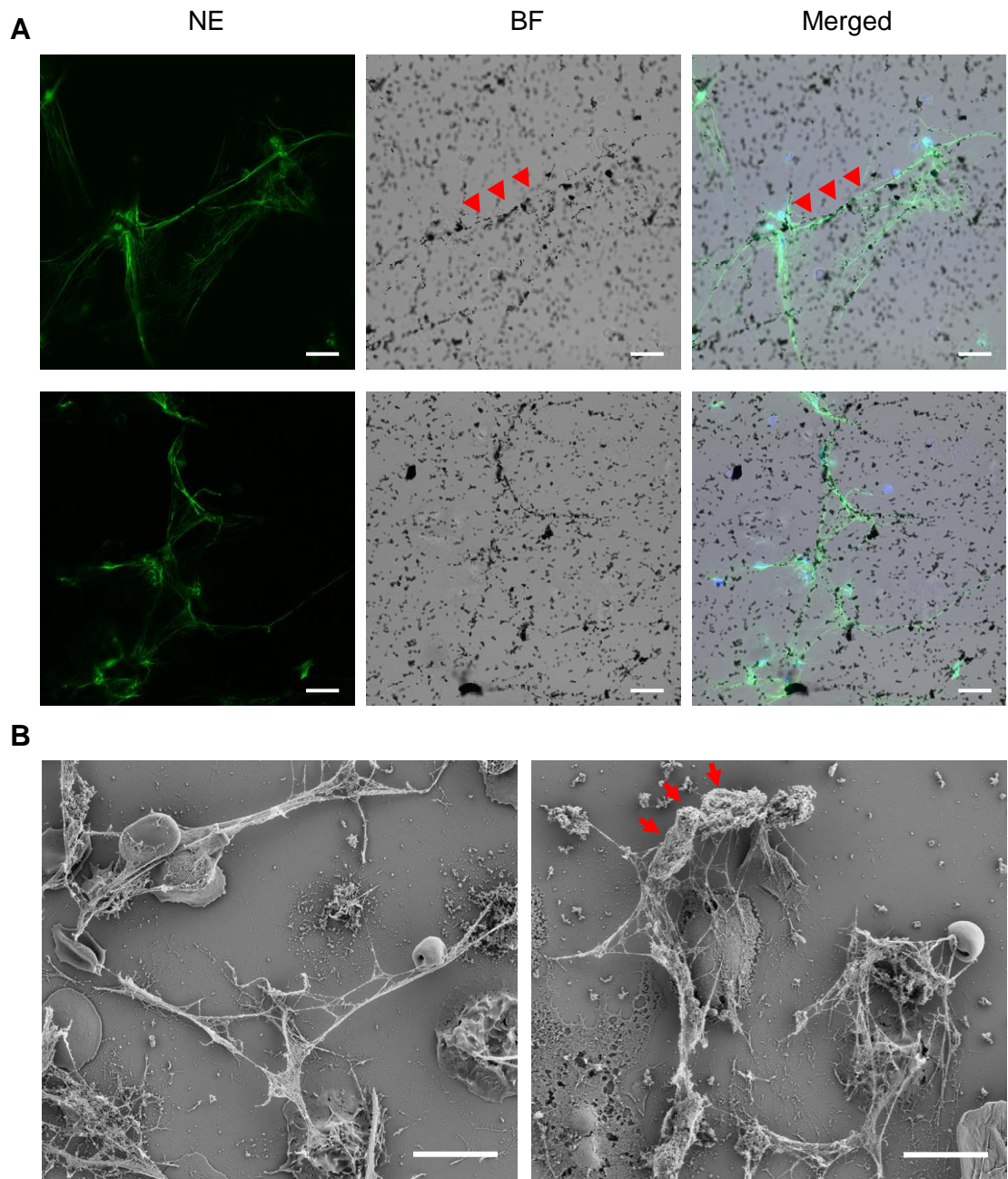
**Figure S3.** Evidence of peroxyntirite-driven biotransformation of MoS<sub>2</sub>. (A) Visual evidence of biotransformation upon incubation of MoS<sub>2</sub> nanosheets with the peroxyntirite donor, SIN-1 (300 μM) for 3 h. (B) Raman spectroscopy analysis of MoS<sub>2</sub> following incubation with SIN-1. The shift of the Raman bands is indicative of N-doping of MoS<sub>2</sub>.



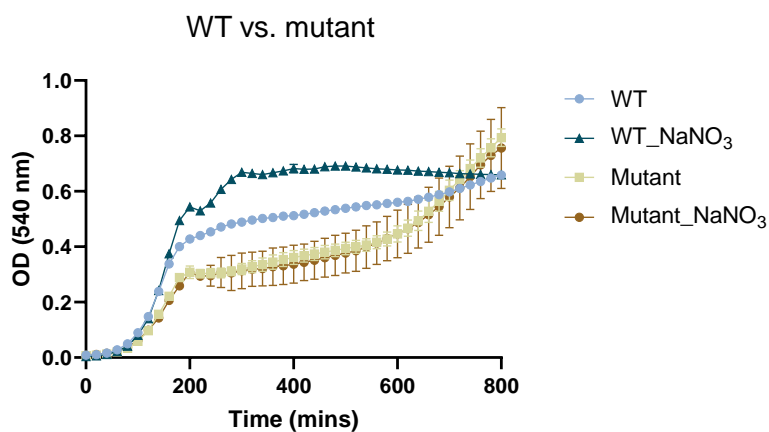
**Figure S4.** NET production in neutrophil-differentiated HL-60 cells. The cells were preincubated with DPI (10  $\mu$ M) and L-NAME (15 mM) for 30 min prior to the exposure to PMA (50 nM), MoS<sub>2</sub> (5 and 50  $\mu$ g/mL), or Na<sub>2</sub>MoO<sub>4</sub> (6.4 and 64  $\mu$ g/mL) for 3 h. NETs were visualized by immunofluorescence staining of NE. DPI (inhibitor of NADPH oxidase) and L-NAME (inhibitor of iNOS) inhibited NETs. Scale bars: 50  $\mu$ m.



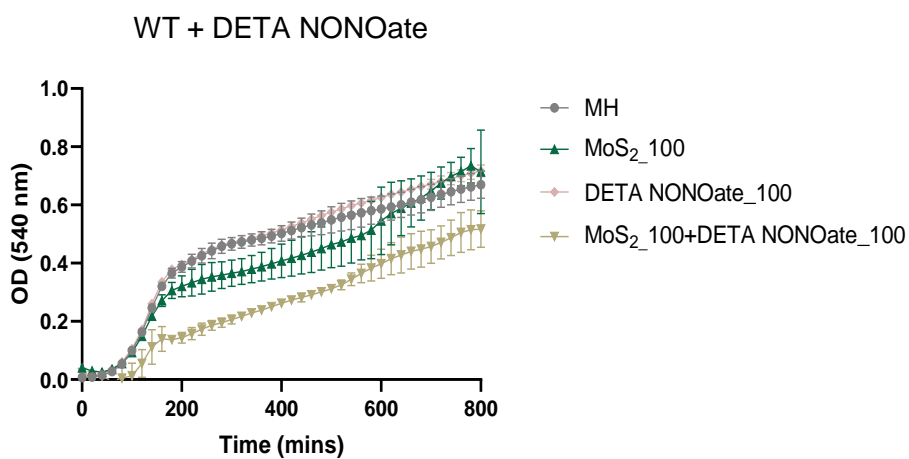
**Figure S5.** 2D-MoS<sub>2</sub> triggered NETs in freshly isolated primary human neutrophils without causing cell death. (A) Cytotoxicity assessment by ATP content. No significant cytotoxicity was observed following a 3-h exposure to PMA (25 nM), MoS<sub>2</sub> and Na<sub>2</sub>MoO<sub>4</sub>. (B) Quantification of NETs release based on extracellular NE activity. Results are normalized to untreated controls and presented as average values ± S.D. from three independent donors. Student's *t*-test was used for the statistical significance compared to controls. \**p*<0.05.



**Figure S6.** NET release in primary human neutrophils. (A) Exposure to MoS<sub>2</sub> (50 µg/mL) for 3 h resulted in release of NETs, and MoS<sub>2</sub> sheets appeared to be attached to NETs (arrows). NETs were visualized by immunofluorescence of NE. BF: bright field. Scale bars: 20 µm. (B) Exposure to PMA (25 nM) (left panel) and MoS<sub>2</sub> nanosheets (50 µg/mL) (right panel) for 3 h resulted in the release of typical web-like NETs as revealed by SEM. The arrows point to possible bundles of MoS<sub>2</sub> nanosheets attached to the chromatin fibers. Scale bars: 10 µm.

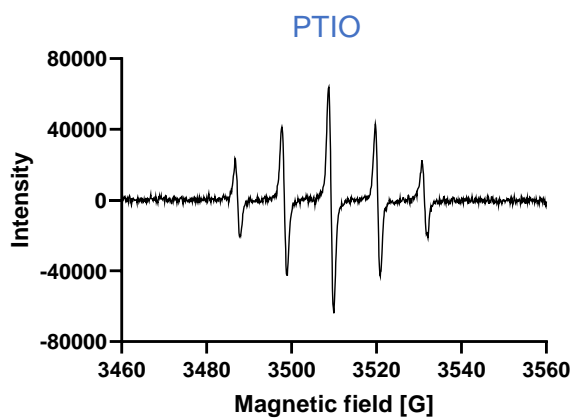
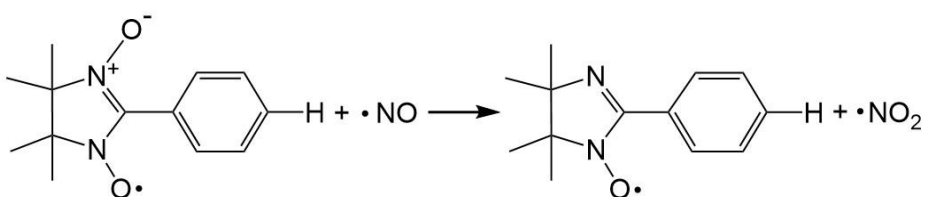


**Figure S7.** Growth curves of the wild-type *E. coli* RK 4353 strain and the RK mutant strain lacking nitrate reductases. The supply of nitrate (NaNO<sub>3</sub>) (10 mM) promoted the growth of wild-type *E. coli* but not the mutant lacking nitrate reductases, as was expected.



**Figure S8.** The addition of the NO donor DETA NONOate (100 μM) plus MoS<sub>2</sub> (100 μg/mL) enhanced the growth inhibition towards wild-type *E. coli* compared to MoS<sub>2</sub> alone.



**A****B**

**Figure S9.** EPR analysis to detect nitric oxide (NO) radicals. (A) EPR spectrum of the spin trap reagent PTIO (100 mM). (B) Reaction of PTIO with NO produces imino nitroxide and nitrogen dioxide.

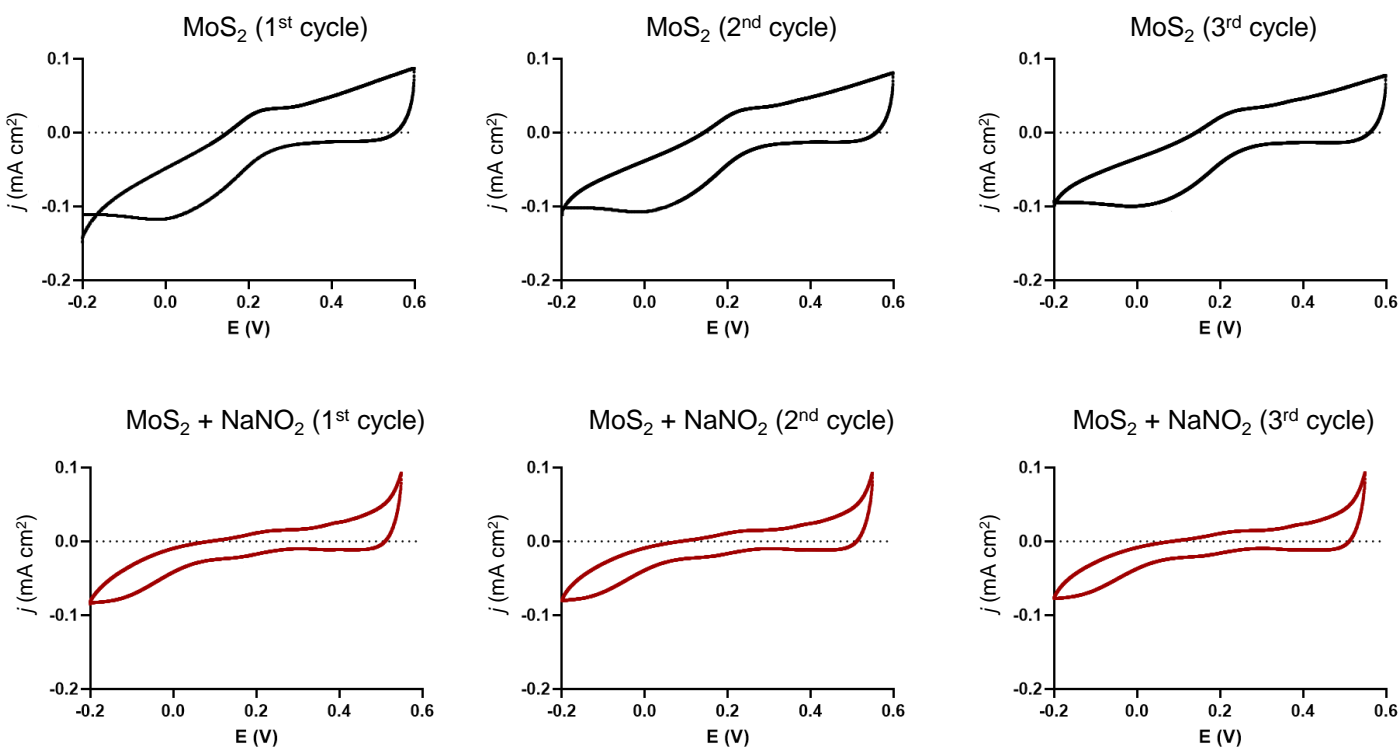


**Figure S10.** Cyclic voltammograms of MoS<sub>2</sub> nanosheets in the absence or presence of nitrite (NaNO<sub>2</sub>). The same results are depicted in Figure 6 (in which all 3 scans are combined in the same figure).